Highly sensitive piezo particulate-polymer foam composites for robotic skin application

Khanbareh, H.; de Boom, K.; van der Zwaag, S.; Groen, W. A.

DOI
10.1080/00150193.2017.1360101

Publication date
2017

Document Version
Final published version

Published in
Ferroelectrics

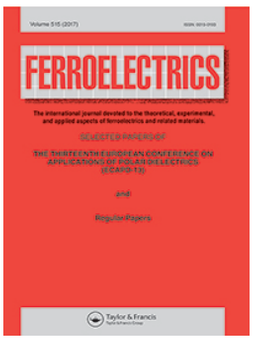

Ferroelectrics

ISSN: 0015-0193 (Print) 1563-5112 (Online) Journal homepage: https://www.tandfonline.com/loi/gfer20

Highly sensitive piezo particulate-polymer foam composites for robotic skin application

H. Khanbareh, K. de Boom, S. van der Zwaag & W. A. Groen

To cite this article: H. Khanbareh, K. de Boom, S. van der Zwaag & W. A. Groen (2017) Highly sensitive piezo particulate-polymer foam composites for robotic skin application, Ferroelectrics, 515:1, 25-33, DOI: 10.1080/00150193.2017.1360101

To link to this article: https://doi.org/10.1080/00150193.2017.1360101

FERROELECTRICS
2017, VOL. 515, 25–33
https://doi.org/10.1080/00150193.2017.1360101

Taylor & Francis
Taylor & Francis Group

Highly sensitive piezo particulate-polymer foam composites for robotic skin application

H. Khanbareh[a,b], K. de Boom[b], S. van der Zwaag[b], and W. A. Groen[b,c]

[a]Materials Innovation Institute (M2i), Delft, The Netherlands; [b]Novel Aerospace Materials Group, Faculty of Aerospace Engineering, Delft University of Technology, Delft, The Netherlands; [c]Holst Center, TNO, Eindoven, The Netherlands

ABSTRACT

Tri-phase PZT-porous polyurethane (PU) composites are investigated with the aim of developing conformable, highly sensitive tactile sensors for application in Human-Machine Interactions. The main goal is to reduce the dielectric constant of the polymer matrix, and improve flexibility of traditional diphase piezo-composites, consisting of ceramic particles in a dense polymeric matrix, by adding a third (gaseous) phase to the system. The presence of the gaseous component in the polymer matrix in the form of well-distributed spherical inclusions effectively decreases the polymer dielectric permittivity, which improves the piezoelectric voltage coefficient of the composites significantly. The unique combination of dielectrophoretic structuring of PZT particles and the addition of a gaseous phase to the polymer resin results in the highest performance of the particulate composite sensors reported in the literature so far. The g_{33} values of the newly developed triphase composites are twice that of the structured di-phase PZT-dense PU composites (80 mV.m/N) and more than five times the g_{33} value of bulk PZT ceramics (24-28 mV.m/N).

ARTICLE HISTORY
Received 21 August 2016
Accepted 12 December 2016

1. Introduction

Several types of polymeric materials can be foamed to low densities for applications that require properties such as weight-reduction, insulation, buoyancy, energy dissipation, mass transport as well as convenience and comfort [1]. More recent advances include polymeric foam scaffolds for tissue engineering [2], shape memory polymer foams for biomedical and aerospace applications [3–6], membranes for gas separation or filtration [7,8], polymeric electrolytes in lithium-ion batteries [9, 10] and hydrogen storage [11, 12].

Recent developments in the field of electronics have encouraged fabrication of ultra-low permittivity dielectrics for the next generations of microchips. They require interlayer of dielectrics with dielectric constants below 2.2. Therefore, a new concept has been developed, based on porous structures, achieved mainly by thermal decomposition of a block copolymer composed of a thermally stable block and a thermally unstable one [13]. These porous

CONTACT H. Khanbareh h.khanbareh@bath.ac.uk
Color versions of one or more of the figures in the article can be found online at www.tandfonline.com/gfer.

materials show a clear relation between decreasing permittivity and increasing porosity. The macroscopic behavior of such polymer foams is determined by a combination of the intrinsic constitutive behavior of the polymeric material, and the microstructure. There are numerous models in literature that relate material properties of the polymer foam to the intrinsic properties of the constituent phases. A simple simulation based on the mixed connectivity model [14], in a serial and a parallel arrangement, can be used to estimate the dielectric properties of the polymer foam. A two-phase dielectric material, consisting of spherical gaseous inclusions in a polymer matrix, is assumed. In the serial mode (0-3), the porosities are homogeneously distributed in the polymer matrix. In the parallel mode (1-3), the microstructure can be considered as the columns of porosity, elongated in the thickness direction. With increasing the gaseous content, the dielectric constant of the polymer foam decreases linearly. However, in a system of homogeneously distributed air inclusions in the polymer matrix, the dielectric constant of the polymer foam decreases exponentially with increasing gaseous content [1, 15]. Therefore, a polymer foam consisting of randomly distributed closed cells, has an effectively reduced dielectric constant compared to the dense polymer.

As far as piezoelectric properties of the ceramic-polymer composite sensors are concerned, optimization of the dielectric properties of the polymer matrix plays an important role in controlling the output voltage of the di-phase composite sensors [16]. The piezoelectric voltage coefficient, g_{33}, is calculated by dividing the d_{33} of the composites by their relative permittivity. Therefore, the piezoelectric performance of the di-phase systems can be enhanced by adding a gaseous phase to the polymer matrix, in form of a homogeneously distributed porosity (0-3 connectivity) to decrease the dielectric constant, while d_{33} is kept unchanged.

Since DEP alignment of piezo particles improves the piezoelectric charge constant of the composites, while foaming significantly decreases the permittivity of the composites, a combination of both will result in enhanced elecetromechanical behavior. The behavior of a tri-phase piezoelectric composite materials is controlled by geometrical, topological, elastic, dielectric, and piezoelectric parameters. In this paper, the influence of topological parameters on the properties of the polyurethane (PU) foam is mapped in detail. Tri-phase composites of PZT-porous PU are manufactured and their functional properties are investigated.

2. Experimental procedure

2.1. Composite manufacturing

Lead zirconate titanate ceramic powder (PZT5A4), provided by Morgan Electro Ceramics, was calcined at 1150°C 1 h in a closed zirconia crucible according to the optimized scheme reported by Van den Ende [17]. After calcination, the powder was dry ball milled for 2 h in a Gladstone-Engineering G90 jar mill. Subsequently, the particles were sieved for 20 min, using a Haver & Boecker EML Digital Plus test sieve shaker with stacked sieves with mesh sizes of 125 μm and 63 μm. The powder was dried for at least 2 h to prevent agglomerations due to moisture, as well as chemical interaction between the polymer and moisture from the particles. The particle size distribution of milled powder in an aqueous solution with 10% isopropyl alcohol, measured by a Beckman Coulter LS230 laser diffraction analyzer, was found to be $d(10) = 0.8$ μm, $d(50) = 1.8$ μm, and $d(90) = 6$ μm.

A two-component urethane rubber, Smooth-on-Econ 80 Polyurethane, is used to serve as the polymer phase in the composites. This polymer is composed of di-isocyanate

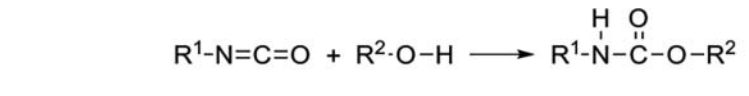

(a) Chemical reaction of di-isocyanates with polyols.

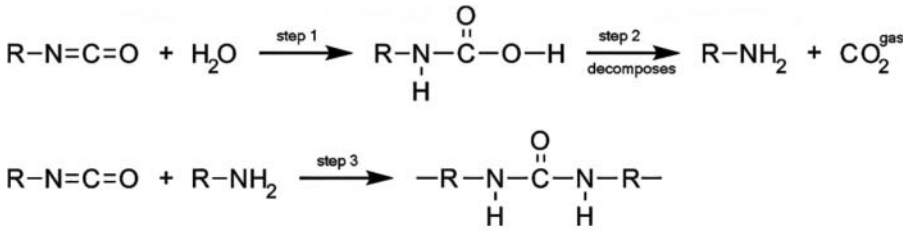

(b) Chemical reaction of di-isocyanates with water and the release of CO_2.

Figure 1. Chemical reaction of PU polymer.

(component A) resin and polyol (component B) was used (see Fig. 1-a). Gas formation is observed upon addition of water to the uncured polymer, due to a chemical reaction between the di-isocyanates component and water, which leads to the formation of poly(urea-urethane), and the release of CO_2 (Fig. 1-b).

To study the effect of demineralised water (D-water) on gas formation in PU, component A was magnetically stirred at 600 RPM for 6-7 min at room temperature. In the meantime, component B and a varying amount of D-water, from 0 to 0.5%, was mixed using a Speedmixer DAC 150.1 FVZ at 3500 RPM for 5 min. Subsequently, component A, B and D-water were magnetically stirred at 600 RPM, until viscosity increased enough to stop the magnet from rotating. A tape-cast-film was made on an aluminum substrate, using a doctor blade that was set at 1 mm. The amount of D-water that was added to 10 mL PU is in the μL range.

Thermogravimetric Analysis (TGA) of the polymer is performed using Perkin Elmer Pyris Diamond at 20°C/min under a nitrogen atmosphere. The results show that, at 200°C, less than 2wt% loss is registered. Subsequently, Differential Scanning Calorimetry (DSC) was performed, at a heating rate of 20°C/min under a nitrogen atmosphere, using the Perkin Elmer Sapphire to find the glass transition temperature, T_g, of −7.6°C. The T_g of the polymer does not appear to be significantly affected by post curing at 100°C.

The production route, that was used for the production of the D-water range of 0 to 0.5%, as explained before, was also used for the production of the first batch of random (0-3) tri-phase composites. However, for the 20 vol% PZT, the initial viscosity of the system due to the presence of the PZT was too high to allow for magnetic stirring. The production route was adapted accordingly. In the new production route, the magnetic stirring step is eliminated. Foams were able to form nonetheless which proves, that PZT particles are able to function as void nucleation sites, thereby replacing the functionality of micro-voids which are introduced by magnetic stirring.

To prepare the composites, PZT particles were dispersed in the mixture of polymer resin and demineralized-water (Dwater) to the specific volume fractions of 0%, 20%, 30% and 40% and mixed at 3500 RPM for 1 min. 0-3 samples were produced by casting the slurry on an aluminum substrate using a doctor blade at the thickness of 1 mm. The surface of the film was exposed to air. Quasi 1-3 samples were produced in a closed mold format using a Teflon mold of 1 mm thick. The details of the mold layout are presented elsewhere [18].

For random and structured samples, the optimum volume fraction of D-water, resulting in maximum reduction of dielectric constant of the polymer matrix is found to be 0.4 vol% and 0.2 vol%, respectively. This optimization will be discussed in detail in the following section. The closed mold used in preparation of DEP structured samples restricts the water evaporation from the mixture, therefore, a lower water content of 0.2 vol% results in similar gas content of 60 vol% similarly as in random composites prepared by casting. The dielectrophoretic structuring is performed on uncured composites by applying an electric field of 3 kV/mm at 3 kHz for 1.5 h, using a function generator (Agilent, 33210A) coupled to a high voltage amplifier (Radiant Technologies Inc., T6000HVA-2), until the polymer matrix is fully cured. After curing, flexible films of 1 mm thickness were obtained. The samples were then poled for 2 h, using a Heinzinger 30000-5 30kV DC amplifier, a Haake N3 digital circulating hot oil bath filled with silicone oil and a custom made sample holder at 100°C, 5 kV/mm.

2.2. Measurement procedure

Circular discs of 16 mm were produced, and electrodes were made by sputtering of Gold for 20 min on both sides using a Quorum Q300T D sputter coater. Subsequently, all samples were punched using a 16 mm punch, thereby removing the material at the edges to prevent leakage current. The dielectric constant of the composites was determined using an Agilent 4263B & 16034E - Inductance Capacitance Resistance Meter (LCR) by the parallel plate capacitor method at 1 V and 1 kHz. The d_{33} of the poled samples were determined using the Piezotest PiezoMeter System PM300 - Berlincourt d_{33} meter, under a 10 N static force and a 0.25 N dynamic force at a frequency of 110 Hz. At least three samples of each composite were tested. For microstructural analysis, the samples were sectioned using scissors along the thickness, and the cross sections were observed using a field emission-scanning electron microscope (FE-SEM) (JEOL, JSM-7500F).

3. Results and discussion

3.1. Microstructure analysis

3.1.1. Microstructures of PZT-porous PU-polymer composites

The effect of D-water content, ranging from 0 to 0.5%, on the microstructures of PU, is shown in Fig. 2. The SEM images are processed using the Image Processing Toolbox of MATLAB, in order to quantify the gaseous volume fraction, pore size and morphology. The images are binarized, and the area fraction of the gaseous phase, as an indication of the volume fraction of this phase, is subsequently calculated. The results of image processing are used to plot the variation of gas content present in the PU polymer, as a function of volume fraction of D-water in the polymer as shown in Fig. 2. A linear correlation is observed between the gas content and the corresponding water content. Increasing the D-water content results in increasing the gas production in the polymer, which is entrapped in a form of a mostly closed cell structure.

The pore size distribution is quantified in the form of a maximum, minimum and average pore diameter. The diameter is an equivalent circular diameter, calculated by conversion of the pore area to the diameter of a circular pore. The minimum diameter does not show significant changes with increasing the water content. However, the average and maximum diameters

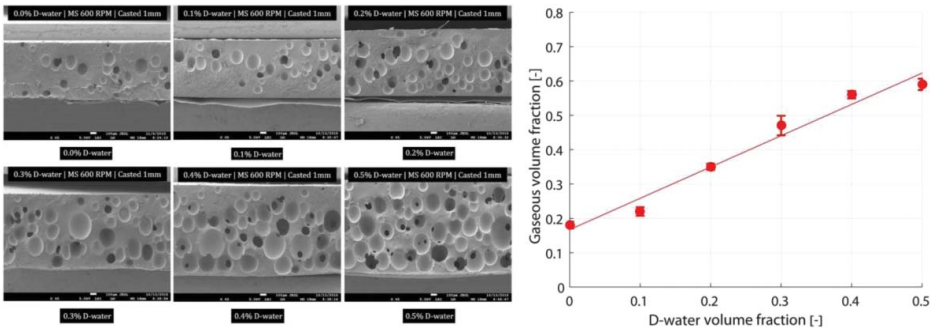

Figure 2. Variation of air content present in neat PU as a function of D-water content.

increase with rising the D-water content from 120 μm to 260 μm and from 250 μm to 429 μm respectively. The 0.5% D-water sample shows the highest average diameter of 260 μm.

The volume fraction of the open cells, observed on the porous-PU microstructures, is calculated using the area fraction of the open cells with respect to the total area of the cells. Increasing the water content from 0% to 0.5% causes the open pore content to vary from 5% to 30%. Increasing the gas volume fraction, leads to cell walls merging that results in a higher content of open cells.

The pore shape is quantified using the aspect ratio, AR, as a measure of elongation, calculated by dividing the maximum to minimum calipers. AR approaches infinity for a long object, while an isotropic object has AR of 1. The pore AR at different D-water content ranges between 1 and 1.3 which is very close to that of perfect spheres.

The microstructures of random PZT-porous PU composites, containing a range of PZT volume contents from 0 to 40%, are shown in Fig. 3. Samples show a uniform distribution of ceramic particles. Agglomerations are only observed at 40 vol% PZT. Pore free layers of about 300 μm and 100 μm are observed adjacent to the substrate on the 10% PZTporous PU and 20% PZT-porous PU microstructures, respectively. The presence of this layer can be attributed to ceramic sedimentation, as well as lower viscosity of the low PZT content samples compared to the magnetically stirred mixtures, as shown in Fig. 2, which is more likely to keep the gas pores entrapped until the polymer matrix is cured. Increasing the PZT volume fraction results in a higher content of interface porosity.

The microstructures of dielectrophoretically (DEP) structured PZT-porous PU foam composites, containing a range of PZT volume content from 0 to 40%, are also shown in Fig. 3. The pores show a uniform distribution through the thickness, likely to be affected by the application of the AC electric field during DEP. The chain formation is clearly visible in the cell walls, especially at lower PZT content. The structured 40% PZT-porous PU sample shows a very rough surface, containing a very high degree of interface porosity.

The variation of gas content, present in the random and structured PZT-porous PU composites is shown in Fig. 4-a. Addition of 0.4% D-water in the random composites of 0, 10% and 20% PZT in PU has successfully resulted in roughly 60 vol% of gas in these samples. In structured composites of 0, 10% and 20% PZT in PU, prepared in a closed mold, addition of 0.2% D-water has resulted in almost 60 vol% of gaseous phase. The structured 30% PZT and 40% PZT-porous

PU samples show very rough cross sections with a high degree of interface porosity which makes the microstructural analysis less accurate. It is presumed that this is the reason for the

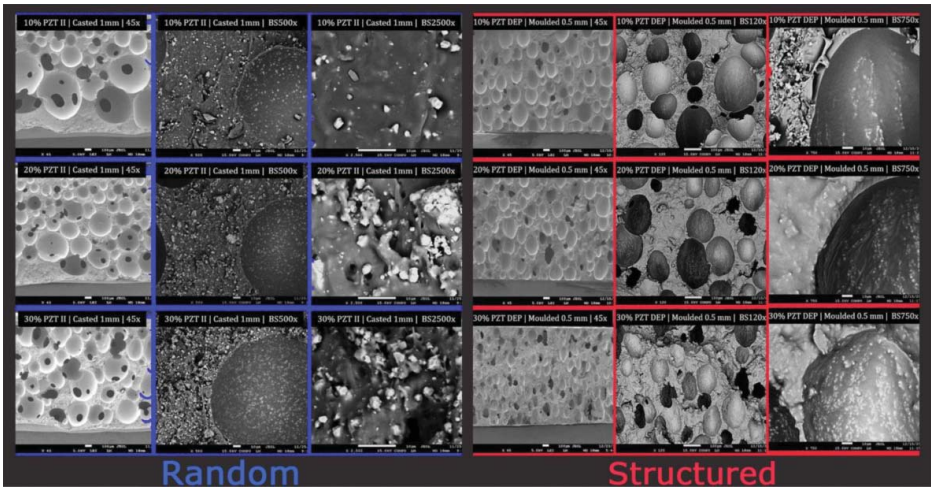

Figure 3. SEM micrographs of the random (0-3) and dielectrophoretically structured (quasi 1-3) tri-phase sample range prepared using 0.4 `*vol*% D-water.

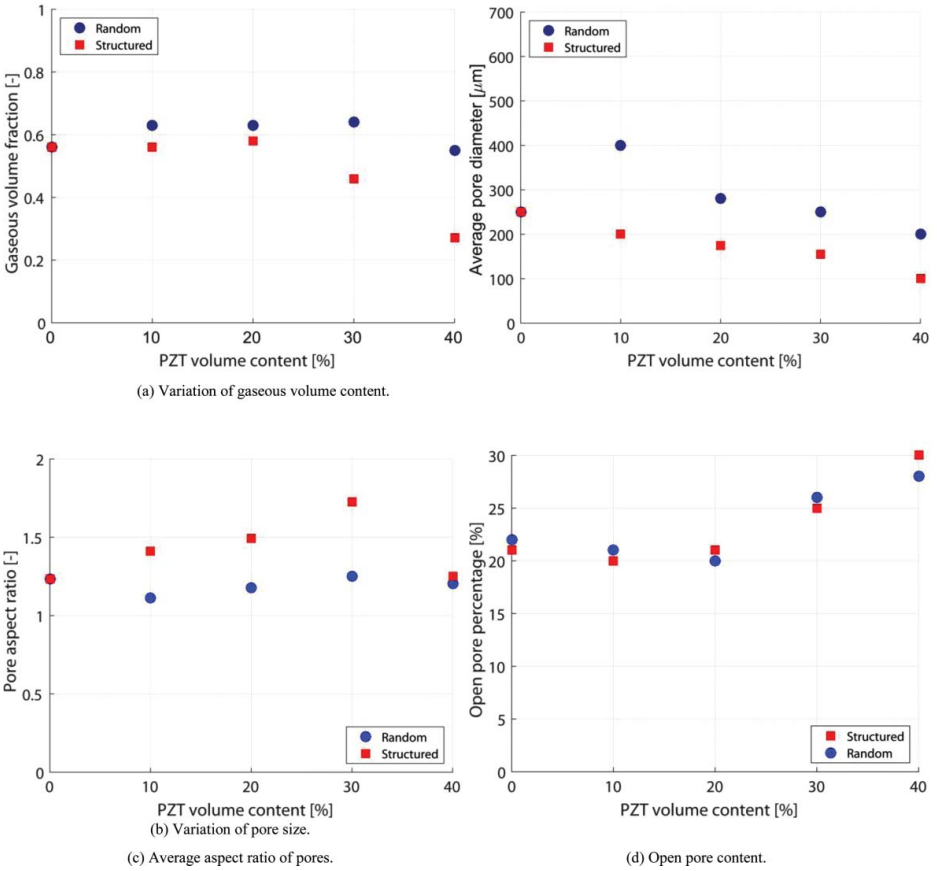

(a) Variation of gaseous volume content.

(b) Variation of pore size.

(c) Average aspect ratio of pores.

(d) Open pore content.

Figure 4. Morphological properties of PZT-porous PU random and structured composites as a function of PZT content.

gas volume content of these two samples, shown in Fig 4-a, to deviate from the expected trend. The average pore diameters, quantified for random and structured PZT-porous PU composites, are presented in Fig 4-b. The average pore size in structured composites varies from 250 μm to 100 μm with increasing the PZT content from 0% to 40%, respectively. Increasing the PZT volume fraction results in higher viscosity of the composites, which restricts the pore growth. The same trend is observed in random composites, containing PZT ranging from 20% to 40%. However, the random 10% PZT-porous PU sample shows an extremely large average pore diameter of 400 μm. The reason can be attributed to the low viscosity of this sample which accommodates the voids on the bottom of the film to merge until they form large pores, while the smaller voids closer to the top escape the film. The aspect ratios of the pores in the random and structured PZT-porous PU composites are shown in Fig 4-c. The random composites of varying PZT content show consistent AR, close to 1, which indicates spherical voids as shown in Fig. 3. However, the DEP structured composites show elongated pores in the field direction, as presented in Fig. 3. A maximum AR of 1.7 is observed for the structured 30% PZT-porous PU composite.

The open pore content as a function of PZT content is shown in Fig 4-d for random and structured composites of PZT and porous PU. Increasing the PZT volume content from 0 to 40% results in a small increase of open pore content, in both random and structured composites. A maximum pore volume fraction of 0.3 is observed for the 40% PZT-porous PU sample.

3.2. Properties of composites

The dielectric constant of the neat PU foam measured at 1 kHz decreases with increasing porosity, as the increasing amount of air ultimately leads to a permittivity of one. The presence of 56 vol% gas results in a 62% reduction in the dielectric constant from 11.1 to 4.2. tan δ of the neat PU foam reduces from 0.13 at 0% gas to 0.09 at 0.6% gas which is in agreement with the documented behavior of polymer foams [13, 19].

Dielectric properties of the structured di-phase and tri-phase composites, containing PZT powder ranging from 0 vol% to 40 vol% in PU polymer foam matrix, are shown in Fig. 5-a. Di-phase PZT-dense PU composites show higher dielectric constant than the tri-phase foam based composites. For the whole PZT range, the improvement in dielectric constant of the tri-phase composites is in accordance with the change in the permittivity of the polymer phase upon addition of the gaseous phase. The piezoelectric charge constant, d_{33}, of the di-phase and tri-phase composites is shown in Fig. 5-b. The maximum d_{33} value of 25 pC/N is obtained for 40% PZT-PU tri-phase composite, which is twice that of the d_{33} value of 40% PZT-epoxy composite [17]. Moreover, adding the gaseous phase results in a decrease in the stiffness of the polymer matrix, which consequently leads to higher d_{33} values compared to a stiffer polymer matrix [16]. A matrix stiffness assures a minimal absorption of mechanical energy by the matrix upon loading. This results in higher effective strains in the piezoelectric composite material. The piezoelectric voltage coefficient, g_{33}, calculated by dividing the d_{33} of the composites by their relative permittivity, is shown in Fig. 5-c. The maximum value obtained for the random composites is 94 mV.m/N, at a PZT volume fraction of 40%, while for the structured porous composite, a value of 166 mV.m/N is obtained at a PZT volume fraction of 10%. At 10 vol%, the maximum g_{33} of a structured dense di-phase composite is approximately 80 mV.m/N. Therefore, a factor of two improvement in g_{33} is obtained in

of 166 mV.m/N is

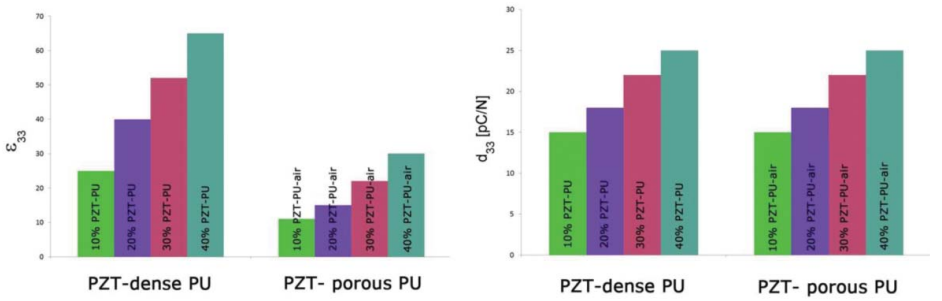

(a) Variation of dielectric constant of PU composites.

(b) Variation of d_{33} of PU composites.

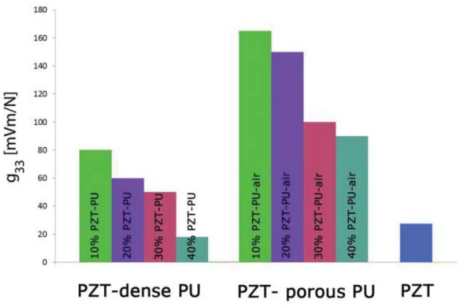

(c) Variation of g_{33} of PU composites.

Figure 5. Dielectric and piezoelectric properties of dense and porous PZT-PU co composites.

10% PZT-porous PU composites by decreasing the dielectric constant of the polymer phase when adding a gaseous content of 60 vol%. The maximum g_{33} reported for structured dense di-phase particulate composites ranges between 70-90 mV.m/N [17,18]. Addition of the third gaseous phase significantly improves the g_{33} performance of the particulate composites.

4. Conclusions

The addition of a gaseous phase in the form of spherical well-distributed inclusions effectively reduces the dielectric permittivity of PU polymer, which improves the piezoelectric voltage coefficient of the PZT-porous PU tri-phase composites significantly. The unique combination of dielectrophoretic structuring of PZT particles and the addition of a gaseous phase to the polymer resin results in the best performance of the particulate composite sensors reported in the literature so far. The g_{33} values of the newly developed triphase composites exceed those of the structured di-phase PZT-dense PU composites (80 mV.m/N), as well as those of the structured PZT-epoxy composites (72-78 mV.m/N) by a factor of two, and more than five times the g_{33} of the bulk PZT ceramics (24-28 mV.m/N).

Funding

This research was carried out under project number M62.3.11438 in the framework of the c (www.m2i.nl).

References

1. K. C. Khemani, *Polymeric Foams*. Washington, DC: American Chemical Society (1997).
2. V. P. Shastri, I. Martin, and R. Langer, Macroporous polymer foams by hydrocarbon templating, *Proceedings of the National Academy of Sciences*, **97**(5), 1970–1975 (2000).
3. Q. Fabrizio, S. Loredana, and S. E. Anna, Shape memory epoxy foams for space applications, *Materials Letters*, **69** 20–23 (2012).
4. L. Santo, F. Quadrini, G. Mascetti, F. Dolce, and V. Zolesi, Mission sts-134: Results of shape memory foam experiment, *Acta Astronautica*, **91** 333–340 (2013).
5. G. Li and M. John, A self-healing smart syntactic foam under multiple impacts, *Composites Science and Technology*, **68**(15-16), 3337–3343 (2008).
6. W. Song, L. Wang, and Z. Wang, Synthesis and thermomechanical research of shape memory epoxy systems, *Materials Science and Engineering: A*, **529** 29–34 (2011).
7. J. Yin and B. Deng, Polymer-matrix nanocomposite membranes for water treatment, *Journal of Membrane Science*, **479** 256–275 (2015).
8. S. Alzahrani and A. W. Mohammad, Challenges and trends in membrane technology implementation for produced water treatment: A review, *Journal of Water Process Engineering*, **4** 107–133 (2014).
9. Q. Xiao, X. Wang, W. Li, Z. Li, T. Zhang, and H. Zhang, Macroporous polymer electrolytes based on pvdf/peob-pmma block copolymer blends for rechargeable lithium ion battery, *Journal of Membrane Science*, **334**(1-2), 117–122 (2009).
10. J. Xi, X. Qiu, J. Li, X. Tang, W. Zhu, and L. Chen, PVDF-PEO blends based microporous polymer electrolyte: Effect of peo on pore configurations and ionic conductivity, *Journal of Power Sources*, **157**(1), 501–506 (2006).
11. G. Banyay, M. Shaltout, H. Tiwari, and B. Mehta, Polymer and composite foam for hydrogen storage application, *Journal of Materials Processing Technology*, **191**(1-3), 102–105 (2007). Advances in Materials and Processing Technologies, July 30th - August 3rd 2006, Las Vegas, Nevada.
12. M. U. Jurczyk, A. Kumar, S. Srinivasan, and E. Stefanakos, Polyaniline-based nanocomposite materials for hydrogen storage, *International Journal of Hydrogen Energy*, **32**(8), 1010–1015 (2007).
13. B. Krause, G.-H. Koops, N. F. van der Vegt, M. Wessling, M. Wubbenhorst, and J. van Turnhout, Ultralow-k dielectrics made by supercritical foaming of thin polymer films, *Advanced Materials*, **14**(15), 1041–1046 (2002).
14. C. Dias, *Ferroelectric composites for pyro- and piezoelectric applications*. PhD thesis, School of electronic engineering and computer systems, University of Wales, Bangor, UK (1994).
15. N. Chand and J. Sharma, Influence of porosity on resistivity of polypropylene foams, *Journal of Cellular Plastics*, **48**(1), 43–52 (2012).
16. S. van Kempen, Optimisation of Piezoelectric Composite Materials Design through Improved Materials Selection and Property Prediction Methods, Master's thesis, Faculty of Aerospace Engineering, Delft University of Technology, Delft The Netherlands (2012).
17. D. A. van den Ende, *Structured piezoelectric composites, materials and applications*. PhD thesis, Faculty of Aerospace Engineering, Delft University of Technology, The Netherlands (2012).
18. H. Khanbareh, S. van der Zwaag, and W. Groen, Effect of dielectrophoretic structuring on piezoelectric and pyroelectric properties of PT-epoxy composites, *Smart Materials and Structures*, **23** (10), 105030 (2014).
19. A. B. Martin Straat, Igor Chmutin, Dielectric properties of polyethylene foams at medium and high frequencies, *Annual Transactions of the Rheology Society*, **18** 1–10 (2010).